STUDIES OF DROPLET BURNING AND EXTINCTION

F.A. Williams
Center for Energy and Combustion Research
Department of Applied Mechanics and Engineering Sciences
University of California San Diego, La Jolla, California 92093

Introduction

A project on droplet combustion, pursued jointly with F.L. Dryer of Princeton University, has now been in progress for many years. The project involves experiments on the burning of single droplets in various atmospheres, mainly at normal atmospheric pressure and below, performed in drop towers (e.g., ref. 1) and designed to be performed aboard space-based platforms such as the Space Shuttle or the Space Station and currently manifest for Spacelab in the MSL-1 flight of the Space Shuttle in April of 1997. It also involves numerical computations on droplet burning, performed mainly at Princeton, and asymptotic analyses of droplet burning, performed mainly at UCSD. The focus of the studies rests primarily on time-dependent droplet-burning characteristics and on extinction phenomena.

The presentation to be given here concerns the recent research on application of asymptotic methods to investigation of the flame structure and extinction of alcohol droplets. These theoretical studies are relevant to the second of the proposed space-flight tests and are currently investigating the extent to which combustion of alcohols can be described by four-step reduced chemistry similar to that which has achieved a good degree of success for alkane flames. These studies have progressed to a point at which a number of definite conclusions can now be stated. These conclusions and the reasoning that led to them are outlined here.

Asymptotic Descriptions of Alcohol Diffusion Flames

A mixture fraction Z, defined to be zero in the oxidizer and unity in the fuel, serves as an attractive independent variable for analyses of diffusion-flame structures because its adoption enables the problem to be formulated in a universal manner that does not depend on the specific geometrical configuration. In the mixture-fraction formulation, the simplest asymptotic description is the Burke-Schumann reaction-sheet structure. This limit corresponds to an infinite Damköhler number for one-step, irreversible chemistry and provides the outer, transport-zone solutions to which the reaction-zone solutions are matched. In the reaction zone there is a one-parameter family of solutions, the parameter being χ_{st}, the value at the stoichiometric mixture fraction Z_{st} of the scalar dissipation rate

$$\chi = 2D|\nabla Z|^2 , \tag{1}$$

where D is the diffusion coefficient of the outer solutions. As χ_{st} increases, the peak temperature decreases, and eventually an abrupt extinction is approached, at a critical value. For droplet burning, it is found that

$$\chi = \frac{8D}{d_l^2}\left\{\frac{[\ln(1-Z)]^2(1-Z)}{\ln(1+B)}\right\}^2 , \tag{2}$$

where d_l is the droplet diameter, and B is the transfer number for the droplet combustion process, given in an approximation of constant specific heat c_p by

$$B = \left\{c_p(T_\infty - T_l) + 2QY_{O_{2\infty}}/(3nW_{O_2})\right\}/L, \tag{3}$$

where T, W, and Y denote temperature, molecular weight, and mass fraction, the subscript ∞ identifies the ambient atmosphere, L is the energy required to vaporize a unit mass of fuel, Q stands for the heat released per mole of gaseous fuel in combustion, and n represents the number of carbon atoms in the alcohol. By use of equation (2) at $Z = Z_{st}$, the droplet diameter at extinction d_{le}, can be obtained from χ_{ste}, the value of χ_{st} at extinction, which has been calculated without reference to the specific geometrical configuration. The calculation employs the reduced chemistry described below.

Reduced Chemistry for Methanol

The starting chemical-kinetic mechanism and the associated rate parameters for methanol are listed in Table 1. The elementary steps and rate parameters given here differ somewhat from those of other studies, since they are based on an evaluation of rate data performed specifically for the present program. In Table 1, CH_2OH stands for the Boltzmann-equilibrated isomers CH_3O and CH_2OH, and the last two sets of rate parameters refer to this mixture. The table represents a minimal set, in the sense that all of the elementary steps shown there are essential.

Introduction of steady-state approximations for all radicals except the important H atom results in a four-step reduced mechanism for the alcohols that can be written as

$$\begin{aligned} &C_nH_{2n+1}OH + \gamma H + \left[\beta - \left(n + 1 + \tfrac{1}{2}\gamma\right)\right]H_2O + \tfrac{1}{2}[3n + \tfrac{1}{2}\gamma \\ &- \beta(1+\alpha)]\,O_2 \rightarrow \beta(H_2 + \alpha CO) + (n - \alpha\beta)\,CO_2 \end{aligned} \tag{I"}$$

$$CO + H_2O \leftrightarrows CO_2 + H_2 \tag{II"}$$

$$2H + M \rightarrow H_2 + M \tag{III"}$$

$$3H_2 + O_2 \leftrightarrows 2H + 2H_2O, \tag{IV"}$$

where α is the number of CO molecules produced per H_2 molecule produced, β is the number of H_2 molecules produced per fuel molecule consumed, and γ, a quantity of critical importance, is the number of radicals destroyed for each fuel molecule consumed. For methanol, this four-step description involves introducing steady-state approximations for CH_2OH, CH_2O, CHO, HO_2, OH and O in Table 1 and results (ref. 2) in $\gamma = 2$, giving a reduced mechanism that can be written as $CH_3OH + 2H \rightarrow 3H_2 + CO$, $CO + H_2O \leftrightarrows CO_2 + H_2$, $2H + M \rightarrow H_2 + M$ and $3H_2 + O_2 \leftrightarrows 2H + 2H_2O$, with corresponding rates $k_{14}C_FC_H$, $(k_9/K_3)C_H(C_{CO}C_{H_2O}/C_{H_2} - C_{CO_2}K_3/K_9)$, $k_5C_MC_HC_{O_2}$ and $k_1C_H[C_{O_2} - (C_H^2C_{H_2O}^2/C_{H_2}^3K_1K_2K_3^2)]$, respectively, where C_i denotes the concentration of species i, subscript F representing the fuel, CH_3OH, and the k's and K's are specific reaction-rate constants and equilibrium constants. Here approximations of partial equilibria have been introduced for steps 2 and 3, and the third-body concentration C_M is weighted with the efficiencies given in Table 1, assuming that only N_2, CO_2 and H_2O are present in significant concentrations in the reaction zone.

Full numerical computations have shown that water-gas equilibrium is an excellent approximation in the reaction zones of these flames, much more accurate than for hydrocarbon

flames, for example. Therefore, the second of the four steps is put into equilibrium, giving $C_{CO} = \alpha C_{H_2}$, where $\alpha \equiv (C_{CO_2}K_3) / (C_{H_2O}K_9)$. There results a three-step mechanism, which can be written as

$$CH_3OH + 2H + \frac{3\alpha - 1}{\alpha + 1} CO_2 \rightarrow \frac{4}{\alpha + 1}(H_2 + \alpha CO) + \frac{3\alpha - 1}{\alpha + 1} H_2O\,, \qquad (I')$$

$$2H + \frac{\alpha}{\alpha + 1} CO_2 \rightarrow \frac{1}{\alpha + 1}(H_2 + \alpha CO) + \frac{\alpha}{\alpha + 1} H_2O \qquad (II')$$

and

$$O_2 + \frac{3}{\alpha + 1}(H_2 + \alpha CO) \rightarrow 2H + \frac{2 - \alpha}{\alpha + 1} H_2O + \frac{3\alpha}{\alpha + 1} CO_2, \qquad (III')$$

with rates $k_{14}C_FC_H$, $k_5C_MC_HC_{O_2}$ and $k_{1f}C_H[C_{O_2} - C_H^2C_{H_2O}^2 / (C_{H_2}^3K_1K_2K_3^2)]$, respectively.

If, in addition, a steady-state approximation for H is introduced, then there results the two-step reduced mechanism

$$CH_3OH + O_2 \rightarrow \left(\frac{1 + 2\alpha}{1 + \alpha}\right) H_2O + \left(\frac{1}{1 + \alpha}\right) CO_2 + \left(\frac{1}{1 + \alpha}\right)(H_2 + \alpha CO)\,, \qquad (I)$$

$$\left(\frac{1}{1 + \alpha}\right)(H_2 + \alpha CO) + \left(\frac{1}{2}\right) O_2 \rightarrow \left(\frac{1}{1 + \alpha}\right) H_2O + \left(\frac{\alpha}{1 + \alpha}\right) CO_2. \qquad (II)$$

The steady-state approximation for H results in

$$C_H = (K_1K_2)^{1/2}K_3C_{O_2}^{1/2}\left(C_{H_2}^{3/2} / C_{H_2O}\right)\left[1 - (k_{14}C_F) / (k_{1f}C_{O_2})\right]^{1/2}, \qquad (4)$$

where $k_5C_MC_{O_2}$ has been neglected in comparison with $k_{14}C_F$ and $k_{1f}C_{O_2}$ because it is quite small in this expression at the pressures considered. The rates of steps I and II are found by reduction of the preceding rates to be

$$\omega_I = k_{14}C_FC_H\,, \quad \omega_{II} = 2k_5C_MC_{O_2}C_H, \qquad (5)$$

in which equation (4) can be used for C_H. This serves to relate the rates to the temperature and the concentrations of the species appearing in steps I and II, as needed in the analysis. In the three-step mechanism, equation (4) is discarded because C_H becomes an additional dependent variable described by an independent differential equation.

The Flame Structure

The flame structure is analyzed by rate-ratio asymptotics (RRA). In the RRA description, there is a thin fuel-consumption zone on the rich side of a broader but still thin layer of H_2 and CO oxidation. This structure is illustrated in figure 1, where δ and ε are small parameters that measure, in the mixture-fraction coordinate, the thicknesses of the fuel-consumption zone and of the oxidation layer, respectively. The fuel-consumption zone, having peak temperature T^0, is located at $Z = Z_0$, a value displaced from Z_{st} by the small amount $\varepsilon\xi_0$, where ξ_0 is calculated in the analysis. This structure is quite similar to that previously determined in the present program for alkane flames, such as heptane; essentially the only difference is the chemistry that occurs in the fuel-consumption zone. The methanol flame is in fact simpler than the alkane flames in that water-gas equilibrium is a much better approximation, so that a three-step description suffices.

The RRA analysis yields the peak temperature as a function of χ_{st}^{-1}, as shown in figure 2. These results are essentially the same for both two-step and three-step descriptions. The minimum value of χ_{st}^{-1} identifies the extinction condition. From these minima, equation (2) can

be used to calculate extinction diameters as functions of the oxygen mole fraction in the atmosphere, as shown in figure 3 for three different values of the atmospheric pressure p. Figure 3 applies for pure methanol droplets that have not absorbed water during burning. In fact, water absorption is significant and modifies extinction conditions, as indicated below.

Effects of Water Dissolution

Water is produced in the flame and dissolves in the liquid fuel as it burns. We have completed an analysis of this effect, treating the gas phase as quasisteady. Two limiting cases were analyzed, namely time-dependent liquid-phase diffusion and perfect liquid-phase mixing. Figure 4 shows results of these analyses for the square of the droplet diameter as a function of time.

It is seen from figure 4 that with time-dependent liquid-phase diffusion the d^2 plots are nearly straight lines. This is because the low diffusion coefficient for water in methanol leads to a relatively small amount of water absorption; the water is contained only in a very thin boundary layer at the liquid surface. On the other hand, with perfect liquid-phase mixing, the d^2 plots are curved, illustrating the reduced vaporization rate as water builds up inside the liquid. These curved lines are seen to be in better agreement with experiment. It is therefore concluded that the experiments involved an appreciable amount of liquid-phase mixing. This same conclusion was reached independently by Dryer and co-workers, on the basis of numerical integrations. The agreement in the conclusion from the two different approaches is a strong indication that the conclusion is correct.

The water absorption also influences flame extinction, a further point of agreement with Dryer et al. In the present approach, since the gas phase is quasisteady, calculating extinction conditions entails calculating extinction diameters for droplets consisting of water-methanol mixtures with different percentages of water. For example, figure 5 shows predicted extinction diameters for droplets consisting of 50% water and 50% methanol on a mass basis. These diameters are seen to be appreciably larger than those in figure 3. Figure 6 illustrates how to determine extinction conditions with time-dependent water absorption. Basically, the droplet diameter and the extinction diameter are plotted as functions of time, and extinction occurs when these two diameters become equal. The resulting extinction predictions are in good agreement with experiment.

Future Plans

The research by asymptotics on methanol droplet combustion is essentially completed. It is intended to spend a little time looking at the kinetics of fuel consumption for higher alcohols, to determine the associated values of γ; the kinetic information needed to do a reasonable job of this has just become available, and so it is a timely investigation. However, most of the future research will involve studying heptane droplet combustion in helium-oxygen atmospheres. This is the system that will be employed in the first flight, MSL-1, and data on this system already are available from preliminary drop-tower tests. Most of the future work, for the next year or two at least, will therefore concentrate on this system. Data on histories of droplet and flame diameters and on extinction conditions will be reduced and compared with our previous theoretical predictions. Data on intensity profiles of emissions in OH bands also will be addressed, to determine what information that data can provide on flame structure, to be compared with theory. The general intent will be to improve understanding of heptane droplet combustion.

References

1. Choi, M.Y., Dryer, F.L, Card, J.M., Williams, F.A., Haggard, J.B., Jr., and Brorowski, B.A., "Microgravity Combustion of Isolated n-Decane and n-Heptane Droplets," AIAA Paper No. 92-242, January 1992.
2. Zhang, B.L., Card, J.M., and Williams, F.A., "Application of Rate-Ratio Asymptotics to the Prediction of Extinction for Methanol Droplet Combustion," Combustion and Flame, to be submitted, 1995.

Table 1
The Starting Chemical-Kinetic Mechanism
and the Associated Rate Parameters
in the form $k = AT^n \exp(-E/R^0T)$

No.[a]	Reactions	A[a]	n[a]	E[a]
	Hydrogen-Oxygen Chain			
1f	$H + O_2 \rightarrow OH + O$	3.52×10^{16}	-0.7	17070
1b	$OH + O \rightarrow H + O_2$	1.15×10^{14}	-0.324	-175
2f	$H_2 + O \rightarrow OH + H$	5.06×10^{4}	2.67	6290
2b	$OH + H \rightarrow H_2 + O$	2.22×10^{4}	2.67	4398
3f	$H_2 + OH \rightarrow H_2O + H$	1.17×10^{9}	1.30	3626
3b	$H_2O + H \rightarrow H_2 + OH$	6.65×10^{9}	1.30	4352
4f	$OH + OH \rightarrow H_2O + O$	$k = 5.46 \times 10^{11} \exp(0.00149T)$		
4b	$H_2O + O \rightarrow OH + OH$	$k = 4.19 \times 10^{7} T^{.58} \exp(0.003T)$		
	Hydroperoxyl Formation and Consumption			
5[b]	$H + O_2 + M \rightarrow HO_2 + M$	6.76×10^{19}	-1.4	0
6	$HO_2 + H \rightarrow OH + OH$	1.70×10^{14}	0.0	874
7	$HO_2 + H \rightarrow H_2 + O_2$	4.28×10^{13}	0.0	1411
8	$HO_2 + OH \rightarrow H_2O + O_2$	2.89×10^{13}	0.0	-497
	Water-Gas Shift			
9f	$CO + OH \rightarrow CO_2 + H$	4.40×10^{6}	1.5	-741
9b	$CO_2 + H \rightarrow CO + OH$	4.97×10^{8}	1.5	21446
	Formyl Formation and Consumption			
10	$CHO + H \rightarrow CO + H_2$	1.00×10^{14}	0.0	0
11[c]	$CHO + M \rightarrow CO + H + M$	2.85×10^{14}	0.0	16795
12	$CH_2O + H \rightarrow CHO + H_2$	2.26×10^{10}	1.05	3278
	Fuel Consumption and Formaldehyde Formation			
13	$CH_2OH + H \rightarrow CH_2O + H_2$	3.00×10^{13}	0.0	0
14	$CH_3OH + H \rightarrow CH_2OH + H_2$	4.00×10^{13}	0.0	6092

[a] Units: mol/lcm^3, K, cal/mol.
[b] Chaperon Efficiencies: N_2, O_2: 1.0, CO: 1.9, CO_2: 3.8, H_2: 2.5, H_2O: 12.0.
[c] Chaperon Efficiencies: same as *b* except H_2O: 16.3

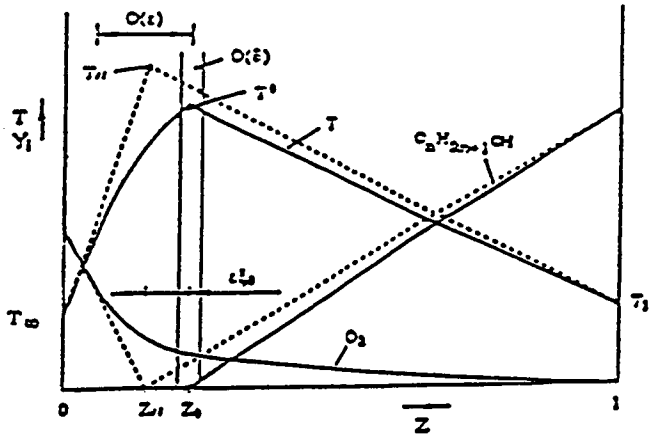

Figure 1 Schematic diagram of the diffusion-flame structure in the mixture-fraction coordinate; dashed lines give the Burke-Schumann structure and solid curves the structure in the two-step approximation.

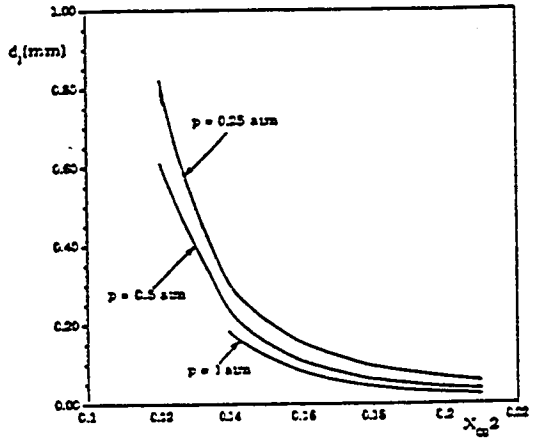

Figure 3 The predicted extinction diameters of pure methanol droplets, burning in oxygen-nitrogen mixtures at 300 K, as functions of the ambient oxygen mole fraction, for three different pressures.

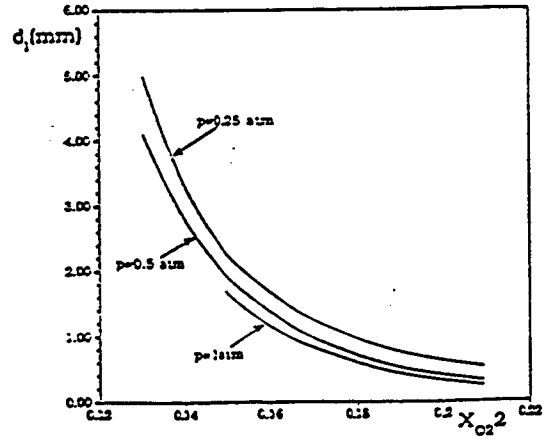

Figure 5 The predicted extinction diameters of droplets composed of 50% methanol and 50% water on a mass basis, burning in oxygen-nitrogen mixtures at 300 K, as functions of the ambient oxygen mole fraction, for three different pressures.

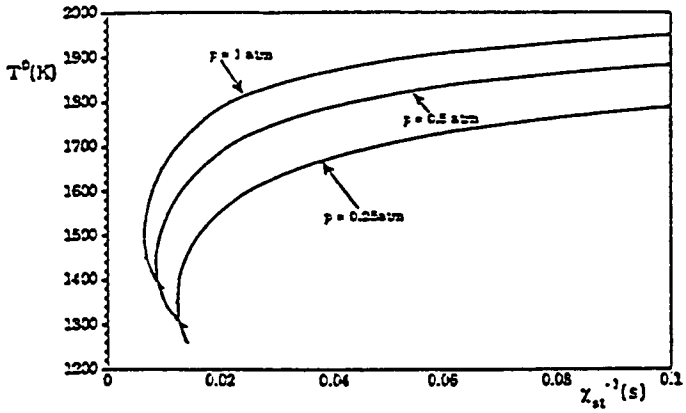

Figure 2 The predicted temperature at the fuel-consumption zone, as a function of the reciprocal of the rate of scalar dissipation at the stoichiometric mixture fraction, for pure methanol droplets burning in air at 300 K, for three different pressures.

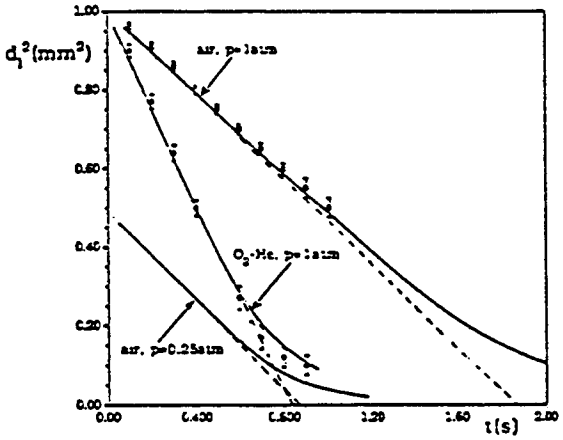

Figure 4 The square of the droplet diameter as a function of time for droplets initially 1 mm in diameter, burning in air at p = 1 atm in a helium-oxygen mixture with $X_{O_2}2$ = 0.5 at p = 1 atm, and for a droplet initially 0.7 mm in diameter, burning in air at p = 0.25 atm; solid lines are for perfect liquid-phase mixing with the present theory, dashed lines are for time-dependent liquid-phase diffusion with the present theory, and points are data from the literature.

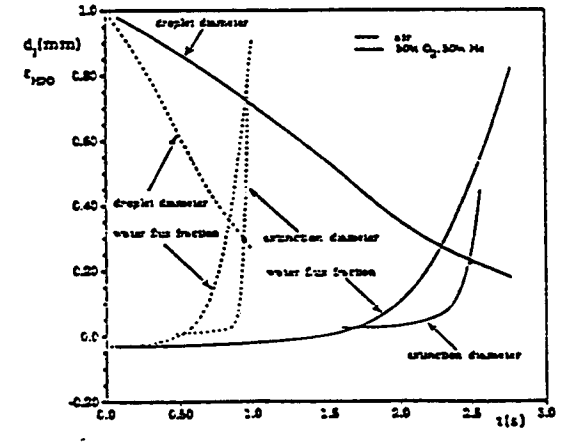

Figure 6 The droplet diameter, the extinction diameter, and the water flux fraction ε_{H_2O} as functions of time with time-dependent water absorption for perfect liquid-phase mixing illustrating how extinction conditions are determined.